

# Nonlinear vibration of functionally graded cylindrical shells: effect of constituent volume fractions and configurations

Matteo Strozzi, Francesco Pellicano

*Department of Mechanical and Civil Engineering, University of Modena and Reggio Emilia, v. Vignolese 905, 41100 Modena, Italy*  
*E-mail: [matteo.strozzi@unimore.it](mailto:matteo.strozzi@unimore.it), [francesco.pellicano@unimore.it](mailto:francesco.pellicano@unimore.it)*

*Keywords:* Nonlinear vibrations, functionally graded materials, shells.

**SUMMARY.** In this paper, the nonlinear vibrations of functionally graded (FGM) cylindrical shells under different constituent volume fractions and configurations are analyzed. The Sanders-Koiter theory is applied to model nonlinear dynamics of the system in the case of finite amplitude of vibration. The shell deformation is described in terms of longitudinal, circumferential and radial displacement fields. Simply supported boundary conditions are considered. Displacement fields are expanded by means of a double mixed series based on Chebyshev orthogonal polynomials for the longitudinal variable and harmonic functions for the circumferential variable. Both driven and companion modes are considered, allowing for the travelling-wave response of the FGM shell. The functionally graded material considered is made of stainless steel and nickel; the properties are graded in the thickness direction, according to a real volume fraction power-law distribution. In the nonlinear model, the shells are subjected to an external radial excitation. Nonlinear vibrations due to large amplitude excitation are considered. Specific modes are selected in the modal expansions; a dynamical nonlinear system is obtained. Lagrange equations are used to reduce nonlinear partial differential equations to a set of ordinary differential equations, from the potential and kinetic energies, and the virtual work of the external forces. Different geometries are analyzed; amplitude-frequency curves are obtained. Convergence tests are carried out considering a different number of asymmetric and axisymmetric modes. The effect of the material distribution on the natural frequencies and nonlinear responses of the shells is analyzed.

## 1 INTRODUCTION

Functionally graded materials (FGMs) are composite materials obtained by combining two or more different constituents, which are distributed in the thickness direction in accordance with a volume fraction law. The idea of FGMs was introduced in 1984 by a group of Japanese material scientists. They studied different physical aspects in the vibration characteristics of FGM shells.

Loy et al. [1] analyzed the vibrations of the cylindrical shells made of a functionally graded material, considering simply supported boundary conditions. They found that the natural frequencies are affected by the constituent volume fractions and configurations of the constituent materials. Leissa [2] studied the linear and nonlinear vibrations of cylindrical shells. He considered the fundamental equations of thin shell theory, with particular attention to the circular cylindrical shells. Amabili [3] analyzed the nonlinear theories of doubly curved shells for advanced materials, as FGMs. The elastic strain energy and kinetic energy for heated, functionally graded shells were defined. Pellicano [4] presented a method for analyzing nonlinear vibrations of cylindrical shells having different boundary conditions. Sanders-Koiter nonlinear theory was applied; displacement fields were expanded in terms of harmonic functions and Chebyshev polynomials.

In this paper, the effect of the constituent volume fractions and configurations on the nonlinear vibrations of functionally graded (FGM) cylindrical shells is analyzed. The Sanders-Koiter theory

is applied to model nonlinear dynamics of the system in the case of finite amplitude of vibration. Shell deformation is described in terms of longitudinal, circumferential and radial displacement fields; the theory considers geometric nonlinearities due to the large amplitude of vibration. Simply supported boundary conditions are considered. The displacement fields are expanded by means of a double mixed series based on harmonic functions for the circumferential variable and Chebyshev polynomials for the longitudinal variable. Both driven and companion modes are considered, allowing for the travelling-wave response of the shell.

Numerical analyses are carried out in order to characterize the nonlinear response of the shell; a convergence analysis is carried out to determine the correct number of the modes to be used. The analysis is focused on determining the nonlinear character of response as the material properties vary; in particular, the effect of the constituent volume fractions and the configurations of the constituent materials on the natural frequencies and nonlinear responses of the shells are studied.

## 2 FUNDAMENTAL EQUATIONS OF FUNCTIONALLY GRADED MATERIALS

The material properties  $P_{fgm}$  of FGMs depend on the material properties and volume fractions of the constituent materials, and they are expressed in the form [1]

$$P_{fgm}(T, z) = \sum_{i=1}^k P_i(T) V_{fi}(z) \quad (1)$$

where  $P_i$  and  $V_{fi}$  are the material property and the volume fraction of the constituent material  $i$ ;  $z$  is the radial coordinate along the thickness  $h$  of the shell.

The material properties  $P$  of the constituent materials can be described as a function of the environmental temperature  $T$ (K) by Touloukian's cubic curve relation [1]

$$P_i(T) = P_0(P_{-1}T^{-1} + 1 + P_1T + P_2T^2 + P_3T^3) \quad (2)$$

where  $P_0, P_{-1}, P_1, P_2$  and  $P_3$  are the coefficients of temperature of the constituent materials.

In the case of a FGM thin cylindrical shell, the volume fraction  $V_f$  can be written as [1]

$$V_f(z) = \left(\frac{z+h/2}{h}\right)^p \quad (3)$$

where the power-law exponent  $p$  is a positive real number, with  $(0 \leq p \leq \infty)$ .

Young's modulus  $E$ , Poisson's ratio  $\nu$  and mass density  $\rho$  are expressed as [1]

$$\begin{aligned} E_{fgm}(T, z) &= (E_2(T) - E_1(T)) \left(\frac{z+h/2}{h}\right)^p + E_1(T), \quad \nu_{fgm}(T, z) = (\nu_2(T) - \nu_1(T)) \left(\frac{z+h/2}{h}\right)^p + \nu_1(T), \\ \rho_{fgm}(T, z) &= (\rho_2(T) - \rho_1(T)) \left(\frac{z+h/2}{h}\right)^p + \rho_1(T) \end{aligned} \quad (4)$$

## 3 SANDERS-KOITER NONLINEAR THEORY OF CIRCULAR CYLINDRICAL SHELLS

In Figure 1, a FGM cylindrical shell having radius  $R$ , length  $L$  and thickness  $h$  is represented; a cylindrical coordinate system  $(O; x, \theta, z)$  is considered in order to take advantage from the axial symmetry of the structure, having the origin  $O$  of reference system located at the centre of one end of the circular cylindrical shell. Three displacement fields are represented: longitudinal  $u(x, \theta, t)$ , circumferential  $v(x, \theta, t)$  and radial  $w(x, \theta, t)$ . The variable  $t$  is the time.

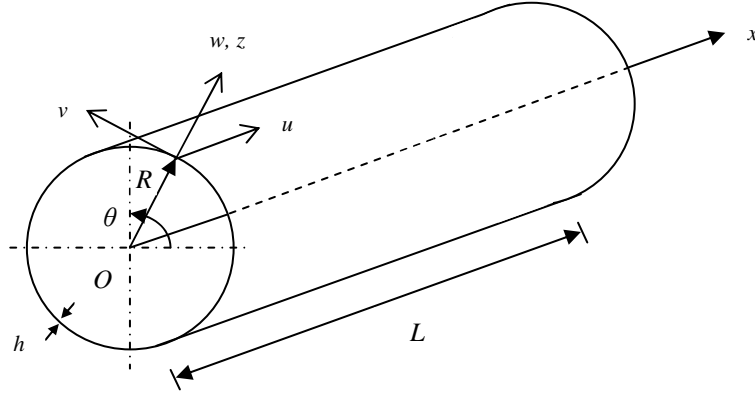


Figure 1: Coordinate system of a functionally graded circular cylindrical shell.

### 3.1 Elastic strain energy, kinetic energy and virtual work of the external forces

The Sanders-Koiter theory of circular cylindrical shells, which is an eight-order shell theory, is based on the Love's "first approximation" [2].

The strain components  $(\varepsilon_x, \varepsilon_\theta, \gamma_{x\theta})$  at an arbitrary point of the circular cylindrical shell are related to the middle surface strains  $(\varepsilon_{x,0}, \varepsilon_{\theta,0}, \gamma_{x\theta,0})$  and to the changes in the curvature and torsion  $(k_x, k_\theta, k_{x\theta})$  of the middle surface of the shell by the following relationships [2]

$$\varepsilon_x = \varepsilon_{x,0} + zk_x, \quad \varepsilon_\theta = \varepsilon_{\theta,0} + zk_\theta, \quad \gamma_{x\theta} = \gamma_{x\theta,0} + zk_{x\theta} \quad (5)$$

where  $z$  is the distance of the arbitrary point of the shell from the middle surface, and  $(x, \theta)$  are the longitudinal and angular coordinates of the shell, see Figure 1.

The middle surface strains and changes in curvature and torsion are given by [2]

$$\begin{aligned} \varepsilon_{x,0} &= \frac{\partial u}{L\partial\eta} + \frac{1}{2}\left(\frac{\partial w}{L\partial\eta}\right)^2 + \frac{1}{8}\left(\frac{\partial v}{L\partial\eta} - \frac{\partial u}{R\partial\theta}\right)^2 + \frac{\partial w}{L\partial\eta} \frac{\partial w_0}{L\partial\eta}, & \varepsilon_{\theta,0} &= \frac{\partial v}{R\partial\theta} + \frac{w}{R} + \frac{1}{2}\left(\frac{\partial w}{R\partial\theta} - \frac{v}{R}\right)^2 + \frac{1}{8}\left(\frac{\partial u}{R\partial\theta} - \right. \\ & \left. \frac{\partial v}{L\partial\eta}\right)^2 + \frac{\partial w_0}{R\partial\theta}\left(\frac{\partial w}{R\partial\theta} - \frac{v}{R}\right), & \gamma_{x\theta,0} &= \frac{\partial u}{R\partial\theta} + \frac{\partial v}{L\partial\eta} + \frac{\partial w}{L\partial\eta}\left(\frac{\partial w}{R\partial\theta} - \frac{v}{R}\right) + \frac{\partial w_0}{L\partial\eta}\left(\frac{\partial w}{R\partial\theta} - \frac{v}{R}\right) + \frac{\partial w}{L\partial\eta} \frac{\partial w_0}{R\partial\theta}, \\ k_x &= -\frac{\partial^2 w}{L^2\partial\eta^2}, & k_\theta &= \frac{\partial v}{R^2\partial\theta} - \frac{\partial^2 w}{R^2\partial\theta^2}, & k_{x\theta} &= -2\frac{\partial^2 w}{LR\partial\eta\partial\theta} + \frac{1}{2R}\left(3\frac{\partial v}{L\partial\eta} - \frac{\partial u}{R\partial\theta}\right) \end{aligned} \quad (6)$$

where  $(\eta = x/L)$  is the nondimensional longitudinal coordinate.

In the case of functionally graded materials, the stresses are related to the strains as follows [1]

$$\sigma_x = \frac{E(z)}{1-\nu^2(z)}(\varepsilon_x + \nu(z)\varepsilon_\theta), \quad \sigma_\theta = \frac{E(z)}{1-\nu^2(z)}(\varepsilon_\theta + \nu(z)\varepsilon_x), \quad \tau_{x\theta} = \frac{E(z)}{2(1+\nu(z))}\gamma_{x\theta} \quad (7)$$

where  $E(z)$  is the Young's modulus and  $\nu(z)$  is the Poisson's ratio (plane stress,  $\sigma_z = 0$ ).

The elastic strain energy  $U_s$  of an isotropic circular cylindrical shell is given by [3]

$$U_s = \frac{1}{2}LR \int_0^1 \int_0^{2\pi} \int_{-h/2}^{h/2} (\sigma_x \varepsilon_x + \sigma_\theta \varepsilon_\theta + \tau_{x\theta} \gamma_{x\theta}) d\eta d\theta dz \quad (8)$$

where  $(h, R, L)$  are the thickness, radius and length of the shell, respectively.

Using equations (5), (7) and (8), the following expression of  $U_s$  can be obtained

$$\begin{aligned}
U_s = & \frac{1}{2}LR \int_0^1 \int_0^{2\pi} \int_{-h/2}^{h/2} \frac{E(z)}{1-\nu^2(z)} \left( \varepsilon_{x,0}^2 + \varepsilon_{\theta,0}^2 + 2\nu(z)\varepsilon_{x,0}\varepsilon_{\theta,0} + \frac{1-\nu(z)}{2}\gamma_{x\theta,0}^2 \right) d\eta d\theta dz + \\
& LR \int_0^1 \int_0^{2\pi} \int_{-h/2}^h \frac{E(z)}{1-\nu^2(z)} \left( \varepsilon_{x,0}k_x + \varepsilon_{\theta,0}k_\theta + \nu(z)(\varepsilon_{x,0}k_\theta + \varepsilon_{\theta,0}k_x) + \frac{1}{2}\gamma_{x\theta,0}k_{x\theta} - \frac{\nu(z)}{2}\gamma_{x\theta,0}k_{x\theta} \right) d\eta d\theta dz + \\
& \frac{1}{2}LR \int_0^1 \int_0^{2\pi} \int_{-h/2}^{h/2} \frac{E(z)}{1-\nu^2(z)} \left( \frac{1}{2}k_{x\theta}^2 + k_x^2 + k_\theta^2 + 2\nu(z)k_xk_\theta + \frac{1-\nu(z)}{2}k_{x\theta}^2 \right) d\eta d\theta z^2 dz + O(h^4) \quad (9)
\end{aligned}$$

where  $O(h^4)$  is a higher-order term in  $h$  according to the Sanders-Koiter theory.

The kinetic energy  $T_s$  of a FGM shell (rotary inertia effect is neglected) is given by [3]

$$T_s = \frac{1}{2}LR \int_0^1 \int_0^{2\pi} \int_{-h/2}^{h/2} \rho(z) (\dot{u}^2 + \dot{v}^2 + \dot{w}^2) d\eta d\theta dz \quad (10)$$

where  $\rho(z)$  is the mass density of the functionally graded shell.

The virtual work  $W$  done by the external forces is written as [3]

$$W = LR \int_0^1 \int_0^{2\pi} (q_x u + q_\theta v + q_z w) d\eta d\theta \quad (11)$$

where  $(q_x, q_\theta, q_z)$  are the distributed forces per unit area acting in longitudinal, circumferential and radial direction, respectively.

#### 4 LINEAR VIBRATION ANALYSIS

In order to carry out a linear vibration analysis, in the present section, the Sanders-Koiter linear theory is considered, i.e. in equation (9) only the quadratic terms are retained.

The displacement fields are expanded by means of a double mixed series: the axial symmetry of geometry and periodicity of deformation in the circumferential direction lead to use harmonic functions, while Chebyshev orthogonal polynomials are considered in the axial direction.

A modal vibration, i.e. a synchronous motion, is obtained in the form [4]

$$u(\eta, \theta, t) = U(\eta, \theta)f(t), \quad v(\eta, \theta, t) = V(\eta, \theta)f(t), \quad w(\eta, \theta, t) = W(\eta, \theta)f(t) \quad (12)$$

where  $u(\eta, \theta, t), v(\eta, \theta, t)$  and  $w(\eta, \theta, t)$  are the displacement fields of the considered system,  $U(\eta, \theta), V(\eta, \theta)$  and  $W(\eta, \theta)$  represent the modal shape, and  $f(t)$  represents the time law, which is supposed to be the same for each displacement field (synchronous motion hypothesis).

The modal shape  $(U, V, W)$  is then expanded in a double mixed series, in terms of Chebyshev polynomials  $T_m^*(\eta)$  and harmonic functions  $(\cos n\theta, \sin n\theta)$ , in the following form [4]

$$\begin{aligned}
U(\eta, \theta) &= \sum_{m=0}^{M_u} \sum_{n=0}^N \tilde{U}_{m,n} T_m^*(\eta) \cos n\theta, & V(\eta, \theta) &= \sum_{m=0}^{M_v} \sum_{n=0}^N \tilde{V}_{m,n} T_m^*(\eta) \sin n\theta, \\
W(\eta, \theta) &= \sum_{m=0}^{M_w} \sum_{n=0}^N \tilde{W}_{m,n} T_m^*(\eta) \cos n\theta \quad (13)
\end{aligned}$$

where  $T_m^*(\eta) = T_m(2\eta - 1)$ ,  $m$  is the number of the longitudinal half-waves,  $n$  is the number of the nodal diameters and  $(\tilde{U}_{m,n}, \tilde{V}_{m,n}, \tilde{W}_{m,n})$  are the generalized coordinates.

#### 4.1 Boundary conditions

In the present work, simply supported circular cylindrical shells are considered; the boundary conditions are imposed by applying constraints to the free coefficients  $(\tilde{U}_{m,n}, \tilde{V}_{m,n}, \tilde{W}_{m,n})$  of the expansions (13). Simply supported boundary conditions are given by [4]

$$w = 0, \quad v = 0, \quad M_x = 0, \quad N_x = 0 \quad \text{for } \eta = (0,1) \quad (14)$$

The previous conditions imply the following equations [4]

$$W(\eta, \theta) = \sum_{m=0}^{M_w} \sum_{n=0}^N \tilde{W}_{m,n} T_m^*(\eta) \cos n\theta = 0, \quad V(\eta, \theta) = \sum_{m=0}^{M_v} \sum_{n=0}^N \tilde{V}_{m,n} T_m^*(\eta) \sin n\theta = 0$$

$$W_{,\eta\eta}(\eta, \theta) = \sum_{m=0}^{M_w} \sum_{n=0}^N \tilde{W}_{m,n} T_{m,\eta\eta}^*(\eta) \cos n\theta = 0, \quad U_{,\eta}(\eta, \theta) = \sum_{m=0}^{M_u} \sum_{n=0}^N \tilde{U}_{m,n} T_{m,\eta}^*(\eta) \cos n\theta = 0 \quad (15)$$

The linear algebraic system given by equations (15) can be solved analytically in terms of the coefficients  $(\tilde{U}_{1,n}, \tilde{U}_{2,n}, \tilde{V}_{0,n}, \tilde{V}_{1,n}, \tilde{W}_{0,n}, \tilde{W}_{1,n}, \tilde{W}_{2,n}, \tilde{W}_{3,n})$ , for  $n \in [0, N]$ .

#### 4.2 Lagrange equations

The equations (12) and (14) are inserted in the expressions of  $T_s$  and  $U_s$  (equations (9 – 10)); a system of ordinary differential equations (ODE) is then obtained by using Lagrange equations.

An intermediate step is the reordering of the variables in a vector [4]

$$q = [\tilde{U}_{0,0}, \tilde{U}_{3,0}, \tilde{U}_{4,0}, \dots, \tilde{U}_{M_u,0}, \tilde{U}_{0,1}, \tilde{U}_{3,1}, \tilde{U}_{4,1}, \dots, \tilde{U}_{M_u,1}, \tilde{V}_{2,0}, \tilde{V}_{3,0}, \dots, \tilde{V}_{M_v,0}, \tilde{V}_{2,1}, \tilde{V}_{3,1}, \dots, \tilde{V}_{M_v,1}, \tilde{W}_{4,0}, \tilde{W}_{5,0}, \dots, \tilde{W}_{M_w,0}, \tilde{W}_{4,1}, \tilde{W}_{5,1}, \dots, \tilde{W}_{M_w,1}] f(t) \quad (16)$$

The maximum number of variables needed for describing a generic vibration mode can be calculated by the following relation  $(N_p = M_u + M_v + M_w - 5)$ ,  $(M_u = M_v = M_w)$  as maximum degree of Chebyshev polynomials, by considering the equations (14) for the boundary conditions.

The number of degrees of freedom of the system can be computed by the following relation  $(N_{max} = N_p \times N)$ , where  $N$  describes the maximum number of nodal diameters considered.

The Lagrange equations for free vibrations read [4]

$$\frac{d}{dt} \left( \frac{\partial L}{\partial \dot{q}_i} \right) - \frac{\partial L}{\partial q_i} = 0, \quad \text{for } i \in [1, N_{max}] \quad (L = T_s - U_s) \quad (N_{max} = N_p \times N) \quad (17)$$

Considering an harmonic motion  $(f(t) = e^{j\omega t})$ , we obtain the secular equation [4]

$$(-\omega^2 \mathbf{M} + \mathbf{K})\mathbf{q} = \mathbf{0} \quad (18)$$

which furnishes frequencies (eigenvalues) and modes of vibration (eigenvectors).

The modal shape, corresponding to the  $j$ th mode, is given by the equations (13), where the coefficients  $(\tilde{U}_{m,n}, \tilde{V}_{m,n}, \tilde{W}_{m,n})$  are substituted with  $(\tilde{U}_{m,n}^{(j)}, \tilde{V}_{m,n}^{(j)}, \tilde{W}_{m,n}^{(j)})$ ;

$$\mathbf{U}^{(j)}(\eta, \theta) = [U^{(j)}(\eta, \theta), V^{(j)}(\eta, \theta), W^{(j)}(\eta, \theta)]^T \quad (19)$$

represents the  $j$ th eigenfunction vector of the original problem.

## 5 NONLINEAR VIBRATION ANALYSIS

In the nonlinear vibration analysis, the full expression of the potential energy (9), containing terms up to the fourth order (cubic nonlinearity), is considered. The displacement fields  $u(\eta, \theta, t)$ ,  $v(\eta, \theta, t)$  and  $w(\eta, \theta, t)$  are expanded by using the linear mode shapes  $U(\eta, \theta), V(\eta, \theta), W(\eta, \theta)$  obtained in the previous section [4]

$$\begin{aligned} u(\eta, \theta, t) &= \sum_{j=1}^{N_{max}} U^{(j)}(\eta, \theta) f_{u,j}(t), & v(\eta, \theta, t) &= \sum_{j=1}^{N_{max}} V^{(j)}(\eta, \theta) f_{v,j}(t), \\ w(\eta, \theta, t) &= \sum_{j=1}^{N_{max}} W^{(j)}(\eta, \theta) f_{w,j}(t) \end{aligned} \quad (20)$$

These expansions respect the simply supported boundary conditions (14); the mode shapes  $U^{(j)}(\eta, \theta), V^{(j)}(\eta, \theta), W^{(j)}(\eta, \theta)$  are known functions expressed in terms of the polynomials and harmonic functions, in which both driven and companion modes are considered, in the form

$$\begin{aligned} U(\eta, \theta) &= \sum_{m=0}^{M_u} \sum_{n=0}^N \tilde{U}_{m,n} T_m^*(\eta) [\cos n\theta + \sin n\theta] + \sum_{m=0}^{M_u} \tilde{U}_{m,0} T_m^*(\eta), \\ V(\eta, \theta) &= \sum_{m=0}^{M_v} \sum_{n=1}^N \tilde{V}_{m,n} T_m^*(\eta) [\sin n\theta + \cos n\theta], \\ W(\eta, \theta) &= \sum_{m=0}^{M_w} \sum_{n=0}^N \tilde{W}_{m,n} T_m^*(\eta) [\cos n\theta + \sin n\theta] + \sum_{m=0}^{M_w} \tilde{W}_{m,0} T_m^*(\eta) \end{aligned} \quad (21)$$

The Lagrange equations for forced vibrations are expressed in the following form [4]

$$\frac{d}{dt} \left( \frac{\partial L}{\partial \dot{q}_i} \right) - \frac{\partial L}{\partial q_i} = Q_i, \quad \text{for } i \in [1, N_{max}] \quad (L = T_s - U_s) \quad (N_{max} = N_p \times N) \quad (22)$$

Expansions (20) are inserted into strain energy (9), kinetic energy (10) and virtual work of external forces (11), in the case of external excitation; using Lagrange equations (22), a system of ordinary differential equations is then obtained.

## 6 NUMERICAL RESULTS

In this section, the nonlinear vibrations of simply supported functionally graded circular cylindrical shells with different constituent volume fractions and configurations are analyzed.

Chebyshev polynomials used in the approximate method have degree equal to  $m = 11$ . The functionally graded material is composed by stainless steel and nickel, its properties are graded in the thickness direction according to a volume fraction distribution, where  $p$  is the considered power-law exponent. The material properties are reported in Table 1 [1].

Table 1: Properties of stainless steel and nickel against coefficients of temperature at (T = 300K).

	stainless steel			nickel		
	$E(\text{Nm}^{-2})$	$\nu$	$\rho(\text{kgm}^{-3})$	$E(\text{Nm}^{-2})$	$\nu$	$\rho(\text{kgm}^{-3})$
$P_0$	$+2.01 \times 10^{11}$	0.326	8166	$+2.24 \times 10^{11}$	0.3100	8900
$P_{-1}$	0	0	0	0	0	0
$P_1$	$+3.08 \times 10^{-4}$	$-2.002 \times 10^{-4}$	0	$-2.79 \times 10^{-4}$	0	0
$P_2$	$-6.53 \times 10^{-7}$	$+3.797 \times 10^{-7}$	0	$-3.99 \times 10^{-9}$	0	0
$P_3$	0	0	0	0	0	0
$P$	$+2.08 \times 10^{11}$	0.318	8166	$+2.05 \times 10^{11}$	0.3100	8900

In the nonlinear model, the following modes having  $m$  longitudinal half-waves and  $n$  nodal diameters ( $m, n$ ) are selected: modes (1,0), (3,0), (1,6) in the longitudinal displacement field; modes (1,6), (1,12), (3,12) in the circumferential displacement field; modes (1,0), (3,0), (1,6) in the radial displacement field. After selecting such modes, each expansion present in equation (20) is reduced to a three-terms modal expansion; the resulting nonlinear system has 9 dofs.

### 6.1 Nonlinear response analysis

The circular cylindrical shell is excited by means of an external modally distributed radial force  $q_r = f_{1,6} \sin \eta \cos 6\theta \cos \Omega t$ , having amplitude of excitation equal to  $f_{1,6} = 0.0012h^2\rho\omega_{1,6}^2$  and frequency of excitation  $\Omega$  close to the (1,6) mode frequency,  $\Omega \cong \omega_{1,6}$ . The driven mode is (1,6), and the external forcing  $f_{1,6}$  is normalized with respect to the mass, acceleration and thickness; the damping ratio is  $\xi_{1,6} = 0.0005$ . In Figure 2, the amplitude-frequency response of a FGM shell with ( $h/R = 0.025, L/R = 20, p = 1$ ) is shown. A softening nonlinear behaviour is observed.

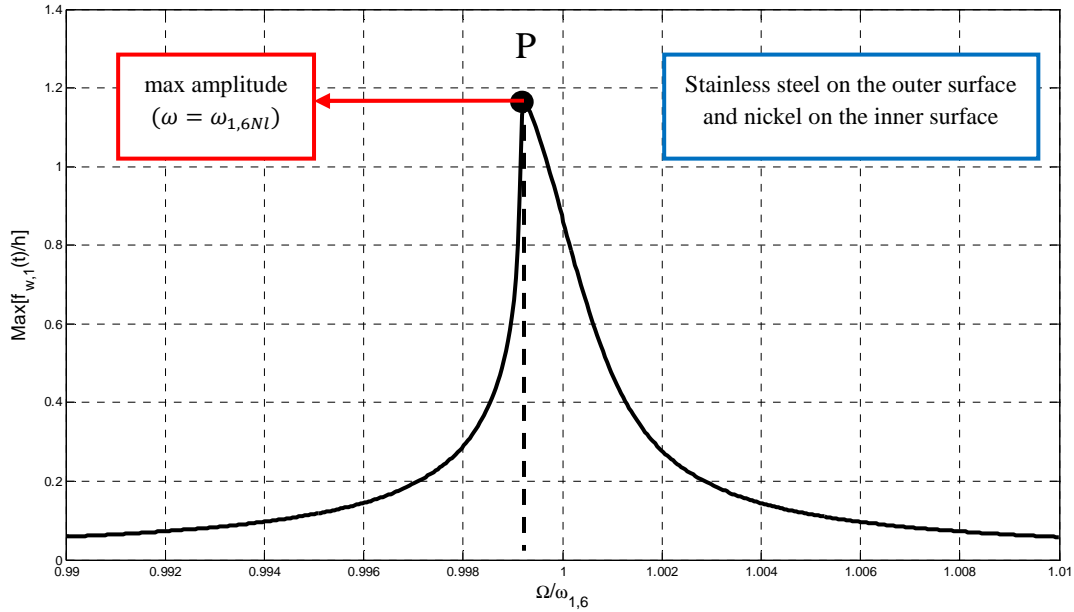


Figure 2: Nonlinear amplitude-frequency curve of the shell ( $h/R = 0.025, L/R = 20, p = 1$ ).

### 6.2 Nonlinear response convergence

The convergence analysis is developed by introducing in longitudinal, circumferential and radial displacement fields a different number of asymmetric and axisymmetric modes: a 6 dof model with modes (1,0), (1,6), (1,12), a 9 dof model with modes (1,0), (3,0), (1,6), (1,12), (3,12), a 12 dof model with modes (1,0), (3,0), (1,6), (3,6), (1,12), (3,12), a 15 dof model with modes (1,0), (3,0), (5,0), (1,6), (3,6), (1,12), (3,12), (1,18), a 18 dof model with modes (1,0), (3,0), (5,0), (7,0), (1,6), (3,6), (1,12), (3,12), (1,18), (3,18) are considered.

In Figure 3, a comparison of nonlinear amplitude-frequency curves of the FGM cylindrical shell ( $h/R = 0.025, L/R = 20, p = 1$ ) is shown: the nonlinear 6 dofs model describes a wrong hardening nonlinear behaviour, the higher-order nonlinear expansions converge to a strongly softening nonlinear behaviour, that is the correct character of the shell response.

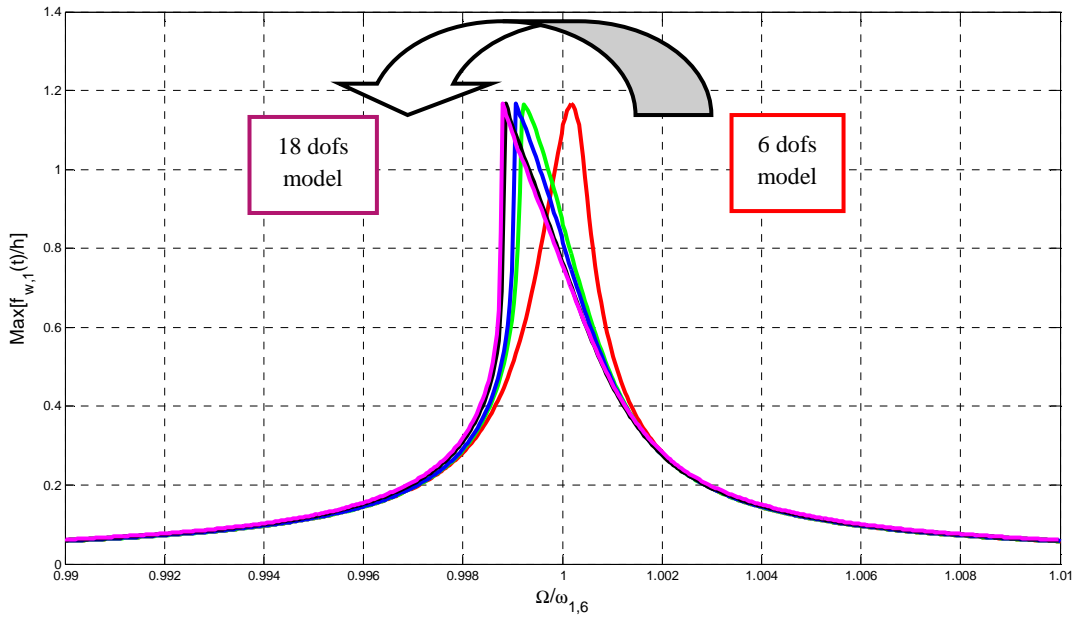


Figure 3: Comparison of nonlinear amplitude-frequency curves ( $h/R = 0.025, L/R = 20, p = 1$ ).  
 —, 6 dofs model; —, 9 dofs model; —, 12 dofs model; —, 15 dofs model; —, 18 dofs model.

### 6.3 Effect of the companion mode participation

In Figure 4, the amplitude-frequency curve with the companion mode participation (i.e. the actual response of the shell) is presented. The response for the mode (1,6) is very similar to the 9-dofs model of Figure 2; the companion mode participation arises around the resonance. Before the exact resonance ( $\Omega = \omega_{1,6}$ ), there is a region where no stable periodic solutions are present: the actual response is then described in terms of pitchfork and Neimark-Sacker bifurcations. The companion mode is not directly excited, and its amplitude is different from zero only for a large amplitude of vibration. The participation of both driven and companion mode gives a travelling wave response moving around the shell: the phase shift between the two coordinates is  $\pi/2$ .



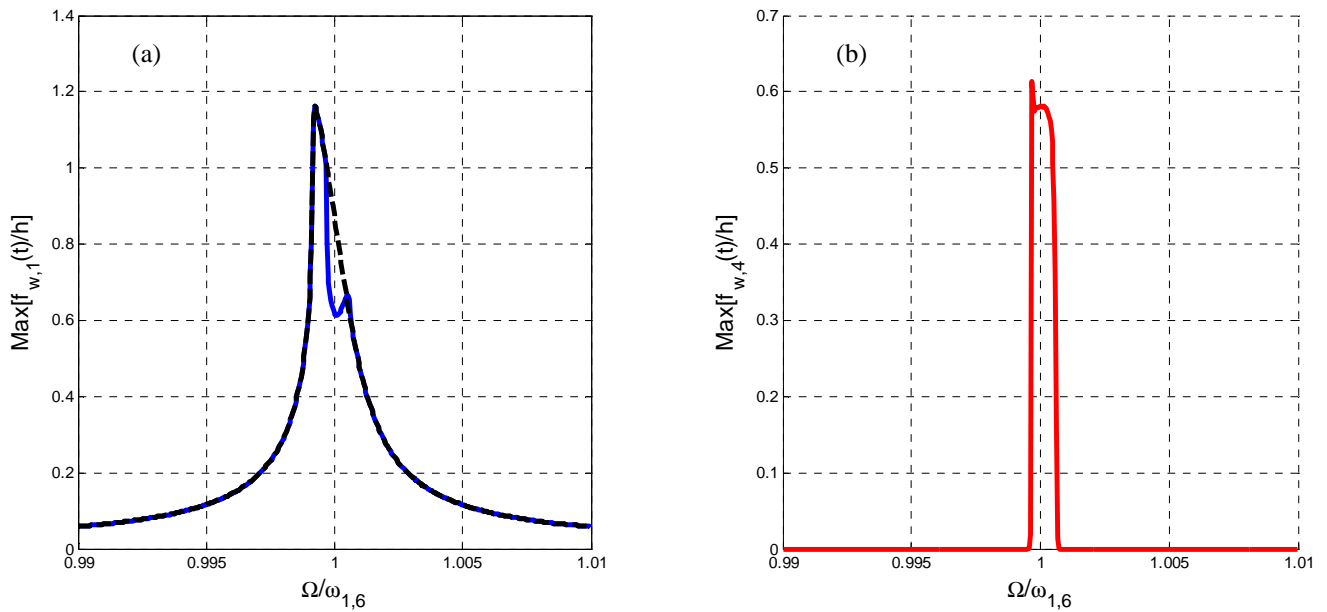


Figure 4: Response-frequency curve with the companion mode participation. (a) Amplitude  $f_{w,1}(t)$  of the driven mode (1,6). (b) Amplitude  $f_{w,4}(t)$  of the companion mode (1,6).

#### 6.4 Effect of the material distribution

The effect of the material distribution on the nonlinear response is analyzed by considering two different FGM shells with ( $h/R = 0.025, L/R = 20$ ): Type I FGM shell, which has nickel on its inner surface and stainless steel on its outer surface, and Type II FGM shell, which has stainless steel on its inner surface and nickel on its outer surface.

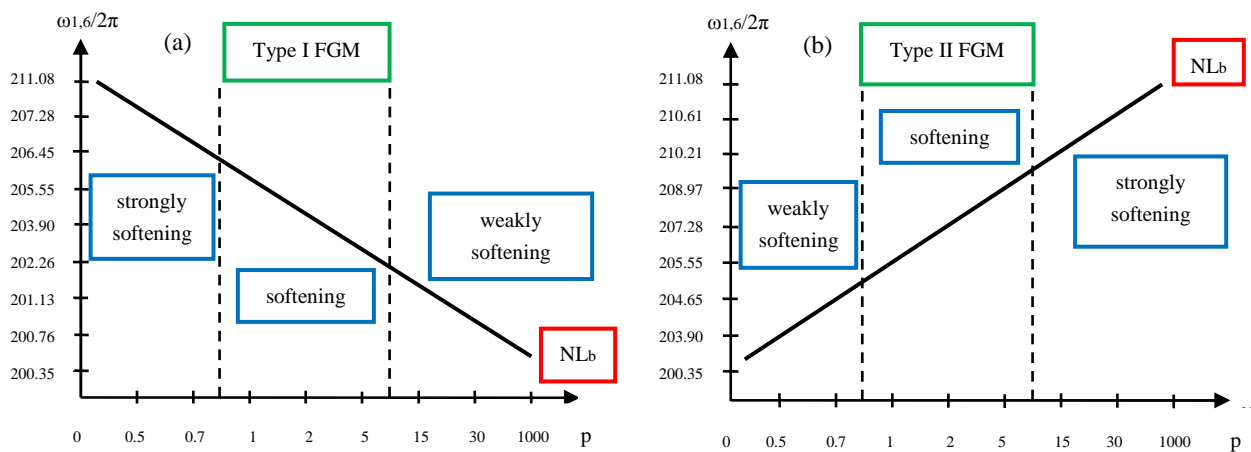


Figure 5: Nonlinear behaviour NLb ( $h/R = 0.025, L/R = 20$ ). (a) Type I FGM; (b) Type II FGM.

In Figure 5(a), the nonlinear behaviour  $NL_b$  of Type I FGM shell is shown: as the value of the exponent  $p$  increases, the value of the natural frequency  $\omega_{1,6}$  decreases, and the behaviour varies from strongly softening ( $p < 1$ ) to weakly softening ( $p > 5$ ). In Figure 5(b), the nonlinear behaviour  $NL_b$  of Type II FGM shell is shown: as the value of the exponent  $p$  increases, the value of the natural frequency  $\omega_{1,6}$  increases, and the behaviour varies from weakly softening ( $p < 1$ ) to strongly softening ( $p > 5$ ).

## 7 CONCLUSIONS

In this paper, the nonlinear vibrations of FGM circular cylindrical shells are analyzed; different configurations and constituent volume fractions are considered. Sanders-Koiter theory is applied to model nonlinear dynamics of the system in the case of finite amplitude of vibration. The shell deformation is described in terms of longitudinal, circumferential and radial displacement fields. Simply supported boundary conditions are considered. Displacement fields are expanded by means of a double mixed series based on harmonic functions for the circumferential variable and Chebyshev polynomials for the longitudinal variable.

Numerical analyses are carried out in order to characterize the nonlinear response of the shells.

A convergence analysis is developed by introducing in longitudinal, circumferential and radial displacement fields a different number of asymmetric and axisymmetric modes; the correct number of modes to describe the actual nonlinear behaviour of the cylindrical shells is determined.

Both driven and companion modes are considered, allowing for the travelling-wave response of the cylindrical shell; frequency-response curves with the companion mode participation (i.e. the actual response of the shell) are obtained.

The influence of the constituent volume fractions and the effect of the configurations of the constituent materials on the natural frequencies and nonlinear responses of the shells are analyzed.

In Type I FGM shell, as the value of the power-law exponent increases, the value of the corresponding natural frequency decreases, and the softening character of the nonlinear behaviour decreases from a strongly softening to a weakly softening behaviour.

In Type II FGM shell, as the value of the power-law exponent increases, the value of the corresponding natural frequency increases, and the softening character of the nonlinear behaviour increases from a weakly softening to a strongly softening behaviour.

### *References*

- [1] Loy, C.T., Lam, K.Y. and Reddy, J.N., "Vibration of functionally graded cylindrical shells", *International Journal of Mechanical Sciences*, **41**, 309-324 (1999).
- [2] Leissa, A.W., *Vibration of Shells*, Government Printing Office, Washington DC (1973).
- [3] Amabili, M., *Nonlinear Vibrations and Stability of Shells and Plates*, Cambridge University Press, New York (2008).
- [4] Pellicano, F., "Dynamic instability of a circular cylindrical shell carrying a top mass under base excitation: Experiments and theory", *International Journal of Solids and Structures*, **48**, 408-427 (2011).